Nonlinear Dynamics and Systems Theory, **17** (1) (2017) 70–85

Shunt Active Power Filter Based Harmonics Compensation of a Low-Voltage Network Using Fuzzy Logic System

A. Morsli [1,2], A. Tlemçani [1*] and M. S. Boucherit [2]

[1] *Laboratoire de Recherche en Electrotechnique et en Automatique (LREA), Université de Médéa, Quartier Ain d'heb 26000, Médéa, Algérie.*
[2] *Laboratoire de Commande des Processus (LCP) Département du Génie électrique, Ecole Nationale Superieure Polytechnique d'Alger 10, avenue Pasteur, Hassan Badi, BP 182, El Harrach, Alger, Algrie*

Received: March 28, 2016; Revised: January 23, 2017

Abstract: This paper presents the design of optimal fuzzy logic system, controlled a shunt active power filter (sAPF) for harmonics compensation which is injected by non-linear loads. This method is applied to a sAPF based on a threephase voltage converter at two levels. The main contribution of this paper is the use of P-Q method for reference currents calculation by applying fuzzy logic for better active filter current control accuracy. For pulse generation, we use the PWM strategy. The results reflect clearly the effectiveness of the proposed APF to meet the IEEE-519 standard recommendations on harmonic levels. To validate the theoretical part, work simulations under Matlab-Simulink are provided.

Keywords: *fuzzy logic system; P-Q algorithm method; shunt Active Power Filter; Total Harmonic Distortion (THD).*

Mathematics Subject Classification (2010): 93C42, 03B52, 93E11, 93Cxx.

* Corresponding author: mailto:h_tlemcani@yahoo.fr

1 Introduction

The increasing use of control systems based on power electronics in industry involves more and more disturbance problems in the level of the electrical power supply networks. Non-linear electronic components such as diode/ thyristor rectifiers, switched mode power supplies, arc furnaces, incandescent lighting and motor drives are widely used in industrial and commercial applications. These nonlinear loads create harmonic or distortion current problems in the transmission and distribution network. The harmonics induce malfunctions in sensitive equipment, over voltage by resonance and harmonic voltage drop across the network impedance that affect power quality [1].

The controller is the heart of the active power filter and many studies are being conducted in this area recently. Conventional PI voltage and current controllers have been used to control the harmonic current and the dc voltage of shunt APLC. Recently, fuzzy logic controllers (FLC) are used in power electronic system and drive applications [2].

The power switching devices are driven with specific control strategy to produce current able to compensate harmonic and poor power factor load. In this work, we take the inverter supplied with a continuous source controlled by fuzzy logic system in series with p-q algorithm method.

2 Shunt Active Power Filter

The shunt Active Power Filter is a power electronic device based on the use of power electronic inverters (Figure 1). The shunt active power filter is connected in a common point connection between the source of power system and the load system which present the source of the polluting currents circulating in the power system lines. This insertion is realized via low pass filter such as, L, LC or LCL filters [3].

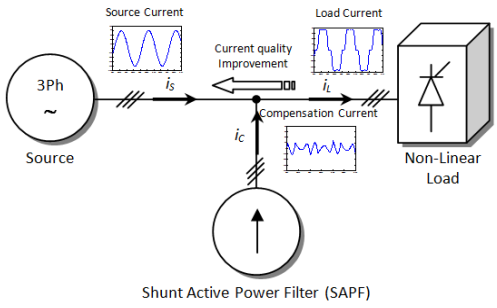

Figure 1: Shunt Active Power Filter principle schematics.

The most important objective of the APF is to compensate the harmonic currents due to the non-linear load. Exactly to sense the load currents and extract the harmonic component of the load current to produce a reference current as shown in Figure 2, The reference current consists of the harmonic components of the load current which the active filter must supply [4,5]. This reference current is fed through a controller and then the switching signal is generated to switch the power switching devices of the inverter, so that the active filter will indeed produce the harmonics required by the load. Finally, the AC supply will only need to provide the load fundamental component, resulting in a low

harmonic sinusoidal supply. A shunt active power filter is controlled to supply/extract compensate current to/from the utility Point Common Coupling (PCC).

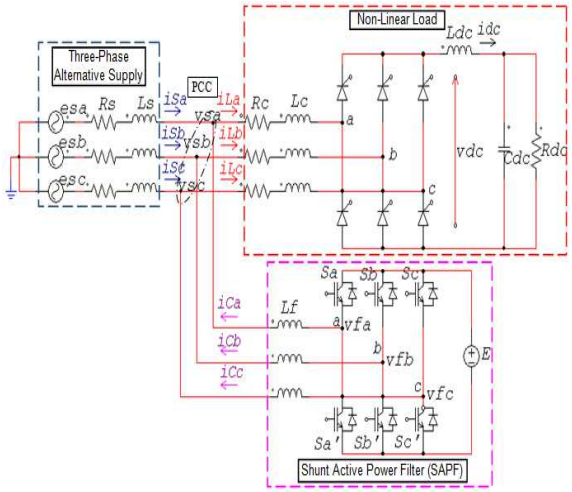

Figure 2: Equivalent schematic of sAPF two levels.

3 Control strategy of the shunt active power filter

The control strategy permits to generate the gating signals to the APF switches. Mainly, we distinguish between two kinds of control techniques. The first one, commonly called the Sigma-Delta Modulation, is based on a hysteresis comparator and is characterized by a non controllable switching frequency. The second one modulates the pulse width and controls the switching frequency: it is called the Pulse width Modulation (PWM). Several PWM techniques exist [6, 7].

Particularly, we cite the carrier-based modulation, the calculated one, and the space vector one. In this paper we applied the carrier-based PWM having the control law described in Figure 3. As shown in Figure 3.a, the pulses (gating signals) are obtained by the intersections of the modulation signal (Δi_C in our case) and one or many carrier signals (generally triangular or saw-toothed signals). This can be realized by comparing the APF error current with the triangular carrier signal (Figure 3.b). After that, the output passes through a hysteresis comparator and is saturated between 0 and 1, corresponding to the two states of the switch. Then, if the saturated output is equal to 1, the leg upper switch is in the 'on' position; else, it is in the 'off' position. Concerning the lower switches, complementarities with the upper ones must be ensured (i.e. Si' = not (Si), i = a, b, c) in order to avoid the opening of voltage sources or the short-cutting of current sources.

In this kind of PWM, the parameters that influence the switching frequency are mainly the modulation index (modulating wave magnitude/carrier signal magnitude) and the carrier frequency.

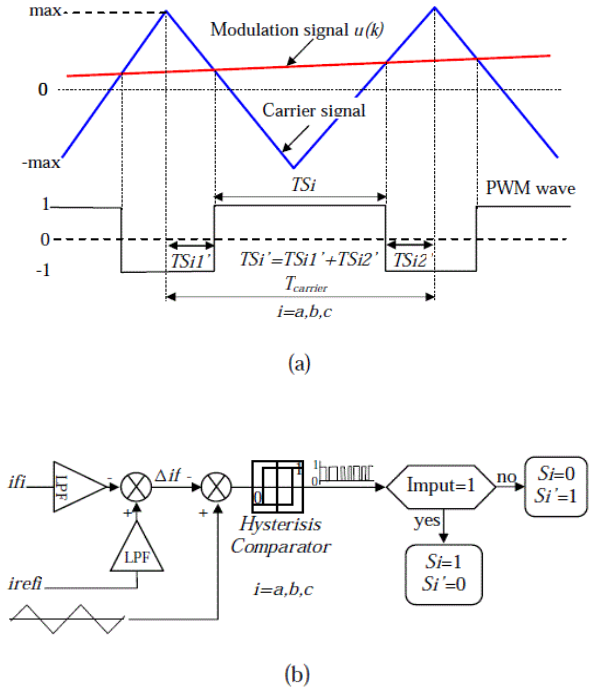

Figure 3: The two-level shunt APF Control law. (a) Carrier-based PWM principle. (b) Pulses generation.

4 Fuzzy Logic Controller

Fuzzy logic serves to represent uncertain and imprecise knowledge of the system, whereas fuzzy control allows taking a decision even if we can not estimate inputs/outputs only from uncertain predicates [8–18]. Figure 4 shows the synoptic scheme of fuzzy controller, which possesses two inputs: the error (e), ($e = i_{ref} - i_C$) and its derivative (de), and one output: the command (cde).

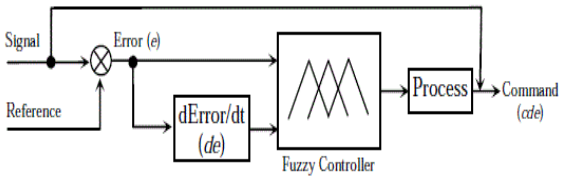

Figure 4: Fuzzy controller synoptic diagram.

Figure 5 illustrates stages of fuzzy control in the considered base of rules and definitions: fuzzification, inference mechanism, and defuzzification.

This step consists of transforming the classical low pass correctors (LPF) on fuzzy ones. The main characteristics of the fuzzy control are:

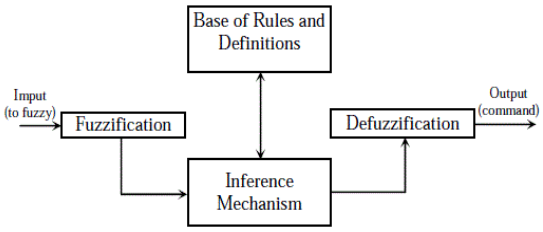

Figure 5: Fuzzy control construction.

- Three fuzzy sets for each of the two inputs (e, de) with Gaussian membership functions.
- Five fuzzy sets for the output with triangular membership functions.
- Implications using the minimum operator, inference mechanism based on fuzzy implication containing five fuzzy rules.
- Defuzzification using the 'centroïd' method.

The establishment of the fuzzy rules is based on the error (e) sign and variation. As explained in Figure 6, and knowing that (e) is increasing if its derivative (de) is positive, constant if (de) is equal to zero, decreasing if (de) is negative, positive if ($i_{Cref} > i_C$), zero if ($i_{Cref} = i_C$), and negative if ($i_{Cref} < i_C$), the command (cde) is:

- zero, if (e) is equal to zero,
- big positive (BP) if (e) is positive both in the increasing and the decreasing cases,
- big negative (BN) if (e) is negative both in the increasing and the decreasing cases,
- negative (N) if (e) is increasing towards zero,
- positive (P) if (e) is decreasing towards zero.

Finally, the fuzzy rules are summarized as follows:

1. If (e) is zero (ZE), then (cde) is zero (ZE).
2. If (e) is positive (P), then (cde) is big positive (BP).
3. If (e) is negative (N), then (cde) is big negative (BN).
4. If (e) is zero (ZE) and (de) is positive (P), then (cde) is negative (N).
5. If (e) is zero (ZE) and (de) is negative (N), then (cde) is positive (P).

The fuzzy inference mechanism used in this work is presented as follows. The fuzzy rules are summarized in Table 1.

$$\mu(u(t)) = \max_{j=1}^{m} [\mu_{A1^j}(e(t)), \mu_{A2^j}(\Delta e(t)), \mu_{B^j}(cde(t))] \tag{1}$$

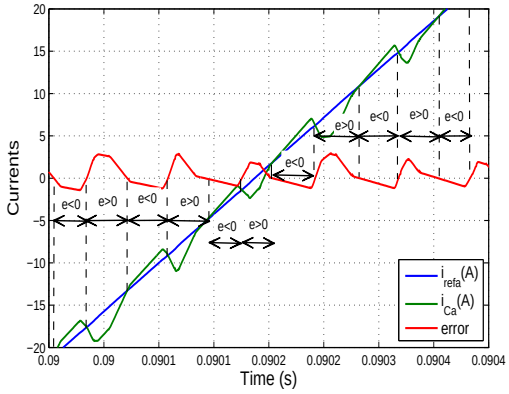

Figure 6: Fuzzy rules establishment.

Fuzzy output $cde(t)$ can be calculated by the center of gravity defuzzification as:

$$cde(t) = \frac{\sum_{i=1}^{m} \mu_B(\mu_i(t)) cde_i}{\sum_{i=1}^{m} \mu_B(\mu_i(t))}, \tag{2}$$

where i is the output rule after inferring [19].

		$e(t)$				
	$cde(t)$	**BN**	**SN**	**Z**	**SP**	**BP**
	BN	BN	BN	SN	SN	Z
	SN	BN	SN	SN	Z	SP
$de(t)$	**Z**	SN	SN	Z	SP	SP
	SP	SN	Z	SP	SP	BP
	BP	Z	SP	SP	BP	BP

Table 1: Fuzzy inference rules.

The following Figure 7 to Figure 10 show FIS editor, FIS file viewer, Surface file viewer Fuzzy and the degree of membership for the error and its derivative and the command signal respectively.

5 Mathematical Model of the Instantaneous Power

5.1 Instantaneous active and reactive powers

This method of identification of harmonic currents is simply to eliminate the dc component of instantaneous active and reactive power which is relatively easy to achieve [20]. Respectively denote the vectors of voltages at the connection point $[v_S]$ and load currents

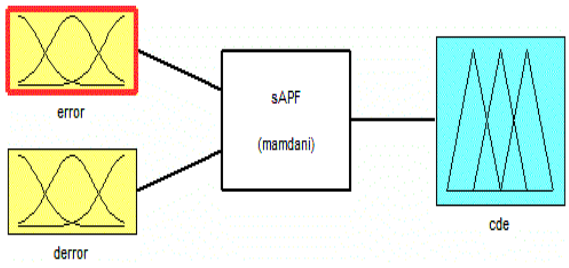

Figure 7: FIS Editor.

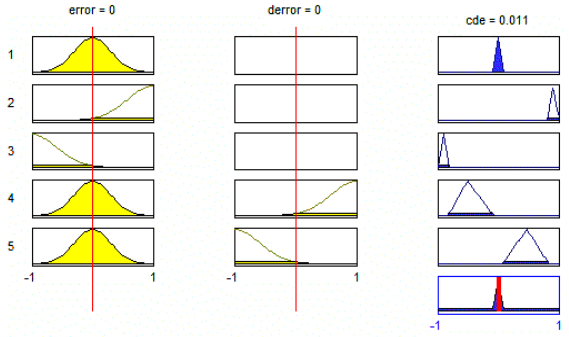

Figure 8: Rule viewer.

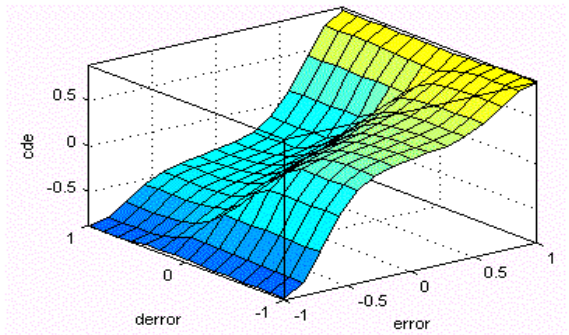

Figure 9: Surface viewer.

$[i_L]$ in a balanced three phase system by:

$$[v_S] = \begin{bmatrix} v_{Sa} \\ v_{Sb} \\ v_{Sc} \end{bmatrix} \tag{3}$$

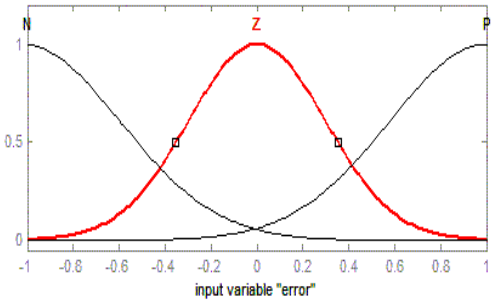

(*a*)

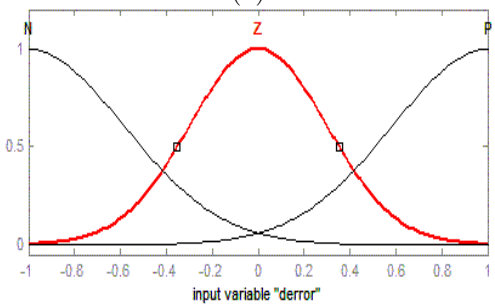

(*b*)

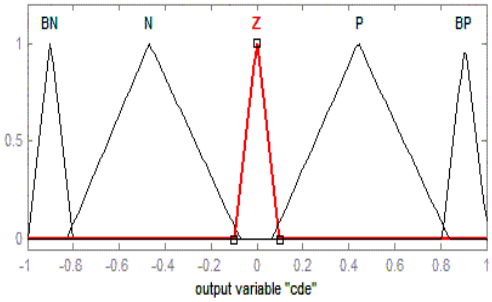

(*c*)

Figure 10: The degree of membership function of fuzzy logic controller for (a) the error, (b) derivative and (c) the command signal.

and

$$[i_L] = \begin{bmatrix} i_{La} \\ i_{Lb} \\ i_{Lc} \end{bmatrix}. \tag{4}$$

The transformation of three-phase instantaneous values of voltage and current in the reference frame of coordinates is given by the following terms:

$$\begin{bmatrix} v_{S\alpha} \\ v_{S\beta} \end{bmatrix} = \sqrt{\frac{2}{3}} \begin{bmatrix} 1 & -1/2 & -1/2 \\ 0 & \sqrt{3}/2 & -\sqrt{3}/2 \end{bmatrix} \begin{bmatrix} v_{Sa} \\ v_{Sb} \\ v_{Sc} \end{bmatrix} \tag{5}$$

and currents :

$$\begin{bmatrix} i_{L\alpha} \\ i_{L\beta} \end{bmatrix} = \sqrt{\frac{2}{3}} \begin{bmatrix} 1 & -1/2 & -1/2 \\ 0 & \sqrt{3}/2 & -\sqrt{3}/2 \end{bmatrix} \begin{bmatrix} i_{La} \\ i_{Lb} \\ i_{Lc} \end{bmatrix}. \tag{6}$$

The real and imaginary instantaneous power denoted p and q are defined by the following matrix relation:

$$\begin{bmatrix} p \\ q \end{bmatrix} = \begin{bmatrix} v_{S\alpha} & v_{S\beta} \\ -v_{S\beta} & v_{S\alpha} \end{bmatrix} \begin{bmatrix} i_{L\alpha} \\ i_{L\beta} \end{bmatrix}. \tag{7}$$

By replacing the two-phase voltages and currents by their counterparts phase, we obtain:

$$p = v_{S\alpha} i_{L\alpha} + v_{S\beta} i_{L\beta} = v_{Sa} i_{La} + v_{Sb} i_{Lb} + v_{Sc} i_{Lc}. \tag{8}$$

Similarly, for the imaginary power we have:

$$q = v_{S\alpha} i_{L\beta} - v_{S\beta} i_{L\alpha} = -\frac{1}{\sqrt{3}}[(v_{Sa} - v_{Sb}) i_{Lc} + (v_{Sb} - v_{Sc}) i_{La} + (v_{Sc} - v_{Sa}) i_{Lb}]. \tag{9}$$

From the expression (8), asking:

$$\triangle = v_{S\alpha}^2 + v_{S\beta}^2,$$

we have :

$$\begin{bmatrix} i_{L\alpha} \\ i_{L\beta} \end{bmatrix} = \frac{1}{\triangle} \left\{ \begin{bmatrix} v_{S\alpha} & -v_{S\beta} \\ v_{S\beta} & v_{S\alpha} \end{bmatrix} \begin{bmatrix} p \\ q \end{bmatrix} \right\} \tag{10}$$

or :

$$\begin{bmatrix} i_{L\alpha} \\ i_{L\beta} \end{bmatrix} = \frac{1}{\triangle} \left\{ \begin{bmatrix} v_{S\alpha} & -v_{S\beta} \\ v_{S\beta} & v_{S\alpha} \end{bmatrix} \begin{bmatrix} p \\ 0 \end{bmatrix} + \begin{bmatrix} v_{S\alpha} & -v_{S\beta} \\ v_{S\beta} & v_{S\alpha} \end{bmatrix} \begin{bmatrix} 0 \\ q \end{bmatrix} \right\} = \begin{bmatrix} i_{L\alpha p} \\ i_{L\beta p} \end{bmatrix} + \begin{bmatrix} i_{L\alpha q} \\ i_{L\beta q} \end{bmatrix} \tag{11}$$

with

$$i_{L\alpha p} = \frac{v_{S\alpha}}{\triangle} p, \quad i_{L\alpha q} = -\frac{v_{S\beta}}{\triangle} q, \quad i_{L\beta p} = \frac{v_{S\beta}}{\triangle} p, \quad i_{L\beta q} = \frac{v_{S\alpha}}{\triangle} q.$$

From the expressions (9), we can write:

$$p = p_{\alpha p} + p_{\beta p} + p_{\alpha q} + p_{\beta q} = p_{\alpha p} + p_{\beta p}. \tag{12}$$

The instantaneous powers p and q are expressed as:

$$p = \overline{p} + \widetilde{p}; \quad q = \overline{q} + \widetilde{q} \tag{13}$$

with:

$\overline{p}$ and $\overline{q}$: Continuous power related to the active and reactive fundamental component of the current.

$\widetilde{p}$ and $\widetilde{q}$: Power alternatives related to the sum of harmonic components of current.

$$\begin{bmatrix} i_{Ca}^* \\ i_{Cb}^* \\ i_{Cc}^* \end{bmatrix} = \sqrt{\frac{2}{3}} \begin{bmatrix} 1 & 0 \\ -\frac{1}{2} & \frac{\sqrt{3}}{2} \\ -\frac{1}{2} & -\frac{\sqrt{3}}{2} \end{bmatrix} \begin{bmatrix} i_{C\alpha}^* \\ i_{C\beta}^* \end{bmatrix}. \tag{14}$$

The diagram in Figure 11 shows the steps for obtaining the current harmonic components of nonlinear load [21].

Figure 12 shows the block diagram of the shunt active power filter controlled by fuzzy logic system with p-q algorithm.

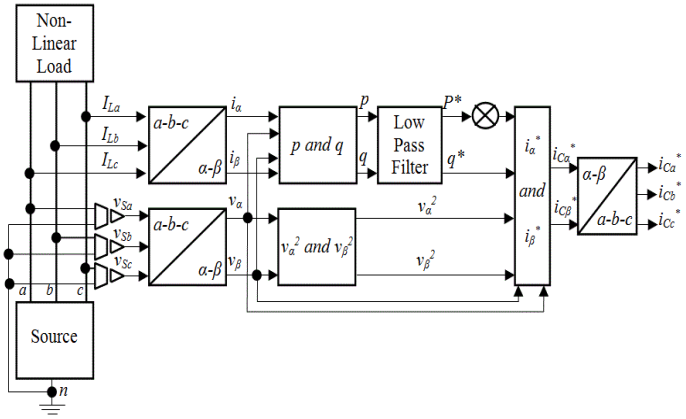

Figure 11: "P-Q" Algorithm extraction of harmonic currents.

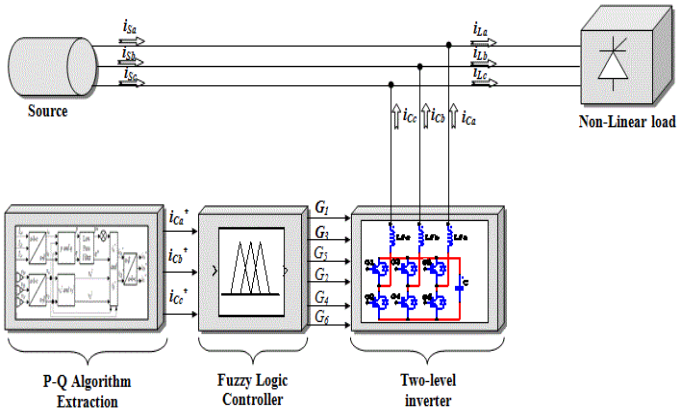

Figure 12: Schematic of a shunt Active Power Filter controlled by a fuzzy logic system.

5.2 Apparent power, reactive power and distortion power

Steady deformed, it must amend the definition of power so that it reflects the current harmonic:

$$S = \sqrt{P^2 + Q^2 + D^2}. \tag{15}$$

Figure 13 shows the vector representation of apparent power.

In single phase, if the instantaneous voltage and current are expressed as:

$$v(t) = \sqrt{2}V_{eff}\sin(\omega t), \tag{16}$$

$$i(t) = \sum_{n=1}^{\infty} \sqrt{2}I_{n,eff}\sin(n\omega t + \phi_n). \tag{17}$$

This is the case for a strong network. Then we have:

$$P = V_{eff}I_{1,eff}\cos(\phi_1), \tag{18}$$

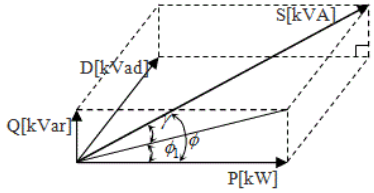

Figure 13: Vector representation of apparent power.

$$Q = V_{eff} I_{1,eff} \sin(\phi_1), \tag{19}$$

$$S = V_{eff} I_{eff}, \tag{20}$$

$$I_{eff} = \sqrt{I_{1,eff}^2 + I_{2,eff}^2 + I_{3,eff}^2 + ... + I_{n,eff}^2}, \tag{21}$$

$$D = V \sqrt{I_{2,eff}^2 + I_{3,eff}^2 + ... + I_{n,eff}^2}. \tag{22}$$

5.3 Total Harmonic Distortion (THD)

Our work focuses on using a parallel active filter, which means we need to calculate the Total Harmonic Distortion of current, as shown in this expression [22]:

$$THD_i = \frac{\sqrt{\sum_{n=2}^{\infty} I_{n(rms)}^2}}{I_{1(rms)}}. \tag{23}$$

6 Simulation Result and Analysis

The SIMULINK toolbox in the MATLAB software is used to model and test the system under steady state and transient conditions before and after using fuzzy logic controller. The system parameters values are summarized in Table 2.

Three-phase network of supply :	
Supply's voltage & frequency,	220 V rms, 50 Hz
Line's inductance Ls & resistance Rs,	19.4 μ H, 0.25 $m\Omega$
Non-linear DC link's :	
InductanceLdc, Resistance Rdc & capacitance Cdc,	20 mH, 6 Ω, 0.01 μF
Inductance L_C & resistance R_C,	0.1 mH, 0.5 Ω
Shunt Active Filter:	
DC supply voltage E, resistance R_f & inductance L_f,	650 V, 4 $m\Omega$, 1.5mH
Control bloc:	
1 st order Low Pass Filter: i_C LPF,	K=1, T= 50 e^{-6}, s
i_{Cref} LPF,	K=1, T = 2 e^{-4}, s
Carrier bipolar saw-toothed, signal magnitude & frequency,	10, 20 kHz
Switching frequency	5 kHz

Table 2: Simulation parameters common to the applications considered.

6.1 Characteristics of the source current before active filtering

The graphs of the source current before application of active filtering are shown in Figures 14, 15 and 16. There is a symmetrical distortion of current i_{La} from the point of half period (Figure 14), which means that the harmonic multiples of 2 and 3 are absent in the spectrum of i_{La} and that only those of rank $(6h \pm 1)$ are present (Figure 15), this is confirmed by the spectrum of i_{La} representing the top 30 most significant harmonics with a THD of 26.37% for an observation period of 0.1 s.

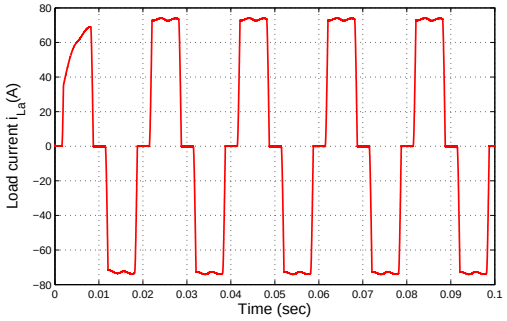

Figure 14: Load current waveform before compensation.

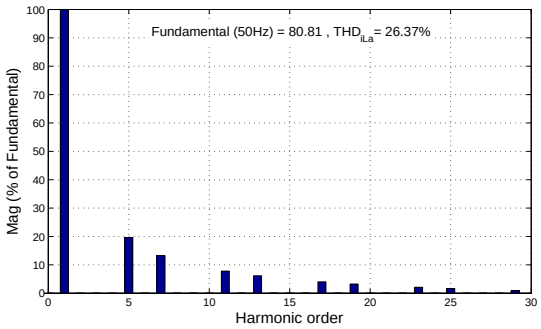

Figure 15: Harmonic spectrum of iLa before compensation.

Harmonic distortion is not the only problem here as Figure 16 shows a degradation in power factor (estimated late 0.0015 s, then $\varphi = 27°$, or $\cos\varphi = 0.891$), so we can expect a change in the reactive energy of the system.

6.2 Characteristics of the source current after active filtering

To improve the waveform i_{Sa}, was inserted an inductance L_C of 0.1 mH and a resistance R_C of 0.5Ω input of the pollutant load with a sAPF, as shown in Figure 2. The result was satisfactory since the distortions have been reduced and it is the same for the THD (I_{Sa}) with a new rate of 2.82%, as shown in Figures 17 and 18.

The source side, the two curves in Figure 19, representing the current and voltage source in phase, despite the presence of a slight delay (delayed i_{Sa} from v_{Sa}) generated

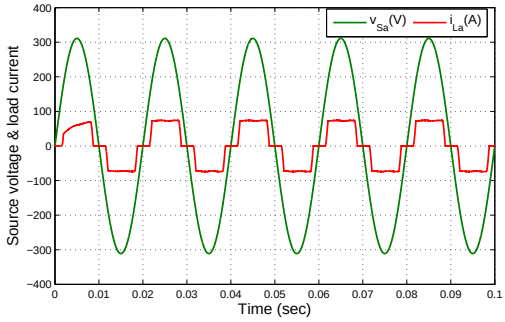

Figure 16: Voltage and current waveforms before compensation.

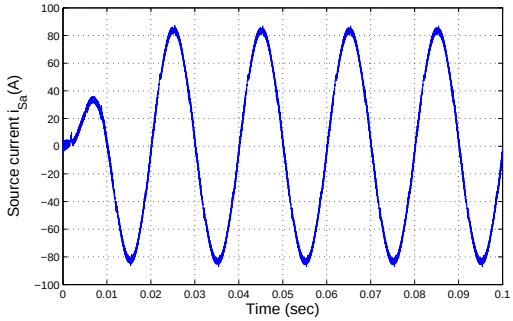

Figure 17: Supply current waveform after compensation.

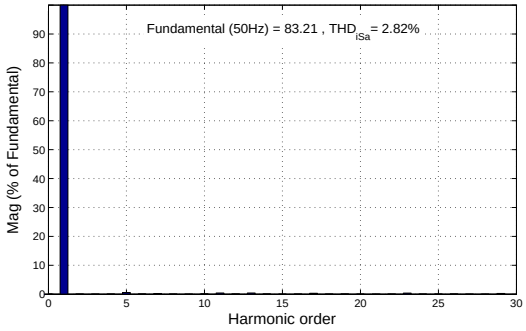

Figure 18: Harmonic spectrum of iSa after compensation.

by L_C and R_C, indicating a power factor corrected, very close to unity. Therefore, so a good compensation of reactive power source.

The deformations in the form of i_{Sa} are in the intersection points nonzero of i_{La} and i_{Ca}, as shown in Figure 20.

The effectiveness of the fuzzy control strategy is illustrated in Figure 21 mentioning the sAPF current pursuing its reference.

Figure 22 gives us an idea about the non-linear DC side current and voltage waveforms

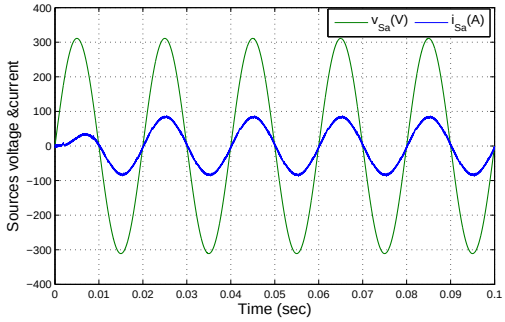

Figure 19: Voltage and current waveforms after compensation.

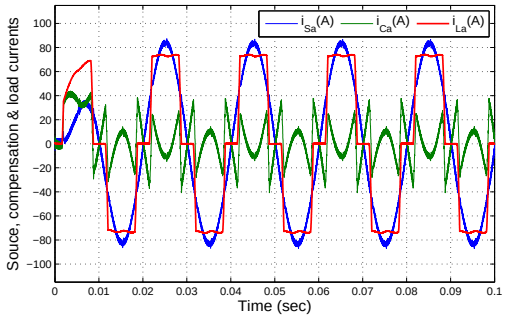

Figure 20: Source current iSa, sAPF filter iCa and non-linear load current iLa.

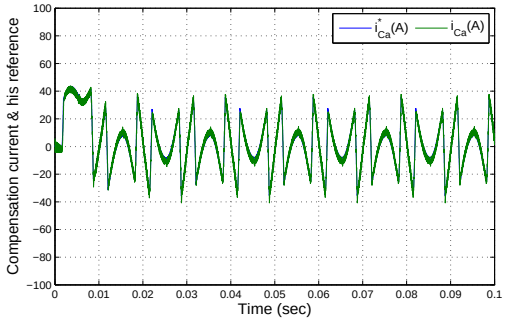

Figure 21: sAPF current and its reference with fuzzy correctors.

with fuzzy controller.

7 Conclusion

The results obtained allow us to visualize the effectiveness of shunt active power filter (sAPF) using a fuzzy controller in series with p-q algorithm method. In fact, the harmonic distortion THD drops from 26.37% to 2.82% after using the active filter. Thus the power factor has been fixed.

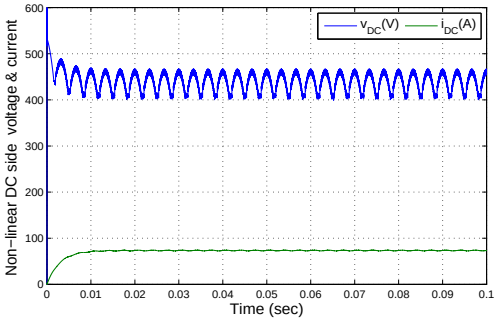

Figure 22: Non-linear DC side current and voltage after compensation.

For future work, we plan to extend our study for other structures by increasing the number of levels of the inverter and compare between them. We also intend to consider a pollution load with more than 26.37% of total harmonic distortion.

References

[1] Morsli, A. OuldCherchali, N. Tlemçani, A. and Boucherit, M. S. Reducing harmonic pollution in low-voltage electrical networks melted on an active conditioner using a five-level inverter npc topology. *International Conference on Automation and Mechatronics CIAM* (2011) 22–24.

[2] Karuppanan, P. and Mahapatra, K. K. With fuzzy logic controller based APLC for compensating harmonic and reactive power. *ACEEE Int. J. on Control System and Instrumentation* **02** (02) (2011) 30–33.

[3] Kouzou, A. Mahmoudi, M. and Boucherit, M. S. Apparent power ratio of the shunt active power filter under balanced power system voltages *Asian Journal of Applied Sciences* **3** (2010) 363–382.

[4] Berbaoui, B. Benachaiba, C. Dehini, R. and Ferdi, B. Optimization of shunt active power filter system fuzzy logic controller based on ant colony algorithm. *Journal of Theoretical & Applied Information Technology* **14** (2010).

[5] Wada, K. Fujita, H. and Akagi, H. Considerations of a shunt active filter based on voltage detection for installation on a long distribution feeder. *Industry Applications Conference, Thirty-Sixth IAS Annual Meeting* **1** (2001) 157–163.

[6] Zhou, K. and Wang, D. Relationship between space-vector modulation and three-phase carrier-based pwm: a comprehensive analysis. *IEEE Transactions on Industrial Electronics* **49** (2002) 186–196.

[7] Benalla, H. and Djeghloud, H. A novel time-domain reference-computation algorithm for shunt active power filters. *ACSE Journal* **6** (2006) 33–40.

[8] Benalla, H. and Djeghloud, H. Shunt active filter controlled by fuzzy logic. *J. King Saud Univ* **18** (2005) 231–247.

[9] Zellouma, L. Saad, S. and Djeghloud, H. Fuzzy logic controller of three-level series active power filter. *EFEEA 10 International Symposium on Environment Friendly Energies in Electrical Applications* (2010) 2–4.

[10] Tlemçani, A., Sebaa, K. and Henini, N. Indirect adaptive fuzzy control of multivariable nonlinear systems class with unknown parameters. *Nonlinear Dynamics and Systems Theory* **14** (2) (2014) 162–174.

[11] Hamidia, F., Larabi, A., Tlemçani, A. and Boucherit, M. S. AIDTC Techniques for Induction Motors. *Nonlinear Dynamics and Systems Theory* **13** (2) (2013) 147–156.

[12] Bentouati, S., Tlemçani, A., Boucherit, M. S. and Barazane, L. A DTC Neurofuzzy Speed Regulation Concept for a Permanent Magnet Synchronous Machine. *Nonlinear Dynamics and Systems Theory* **13** (4) (2013) 344–358.

[13] Tlemçani, A., Chekireb, H. and Boucherit, M. S. A New Robust Adaptive Control of a Class of MIMO Nonlinear Systems with Fuzzy Approximators. *Archive of Control Sciences* **16** (3) (2006) 247–264.

[14] Tlemçani, A., Chekireb, H., Boucherit, M. S. ans Labiod, S. Decentralized direct adaptive fuzzy control of non-linear interconnected MIMO system class. *Archive of Control Sciences* **17** (4) (2007) 357–374.

[15] Tlemçani, A., Chekireb, H., Boucherit, M. S. and Djemai, M. Decentralized Direct Adaptive Fuzzy Control of Permanent Magnet Synchronous Motor. *The Mediterranean Journal of Measurement and Control* **4** (1) (2008) 33–43.

[16] Tlemçani, A., Bouchhida, O., Benmansour, K., Boudana, D. and Boucherit, M. S. Direct Torque control strategy (DTC) based on fuzzy logic controller for a permanent magnet synchronous machine drive. *Journal of Electrical Engineering and Technology* **4** (1) (2009) 66–78.

[17] Barkat, S., Tlemçani, A. and Nouri, H. Non-interacting Adaptive Control of PMSM Using Interval Type-2 Fuzzy Logic Systems. *IEEE Transactions on Fuzzy Systems* **19** (5) (2011) 925–936.

[18] Benzerafa, F., Tlemçani, A. and Sebaa, K. Type-1 and Type-2 Fuzzy Logic Controller Based Multilevel DSTATCOM Using SVM, *Studies in Informatics and Control* **25** (1) (2016) 87–98.

[19] Choe, G.-H. and Park, M.-H. A new injection method for ac harmonic elimination by active power filter. *IEEE Transactions on Industrial Electronics* **35** (1988) 141–147.

[20] Morsli, A. OuldCherchali, N. Tlemçani, A. and Boucherit, M. S. Application of pq algorithm and fuzzy controller to a multilevel inverter as a shunt active power filter. *The International Conference on Electronics & Oil: from theory to applications* (2013).

[21] Akagi, H. Kanazawa, Y. and Nabae, A. Generalized theory of the instantaneous reactive power in three-phase circuits. *IPEC* **83** (1983) 1375–1386.

[22] Czarnecki, L. S. Instantaneous reactive power p-q theory and power properties of three-phase systems. *IEEE Transactions on Power Delivery* **21** (2006) 362–367.